Eurasian Journal of Physics and Functional Materials

Volume 9 | Number 2

Article 6

Pages: 110 - 121

6-30-2025

Development Of A Neutronic Model Of The Wwer-1000 Reactor Facility Core

D.M. Seken
“Institute of Atomic Energy” RSE NNC RK, Kurchatov, Kazakhstan, seken@nnc.kz

A.S. Surayev
“Institute of Atomic Energy” RSE NNC RK, Kurchatov, Kazakhstan

R.A. Irkimbekov
“Institute of Atomic Energy” RSE NNC RK, Kurchatov, Kazakhstan

G.A. Vityuk
“Institute of Atomic Energy” RSE NNC RK, Kurchatov, Kazakhstan

N.Y. Mukhamedov
“Institute of Atomic Energy” RSE NNC RK, Kurchatov, Kazakhstan

See next page for additional authors

Recommended Citation

Seken, D.M.; Surayev, A.S.; Irkimbekov, R.A.; Vityuk, G.A.; Mukhamedov, N.Y.; Zhanbolatov, O.M.; and Vityuk, V.A. (2025) "Development Of A Neutronic Model Of The Wwer-1000 Reactor Facility Core," *Eurasian Journal of Physics and Functional Materials*: Vol. 9: No. 2, Article 6.
DOI: https://doi.org/10.69912/2616-8537.1248

ORIGINAL STUDY

Development of a Neutronic Model of the WWER-1000 Reactor Facility Core

Darkhan M. Seken [a,b,*], Artur S. Surayev [a], Ruslan A. Irkimbekov [a], Galina A. Vityuk [a], Nurzhan Y. Mukhamedov [a], Olzhas M. Zhanbolatov [a], Vladimir A. Vityuk [c]

[a] "Institute of Atomic Energy" RSE NNC RK, Kurchatov, Kazakhstan
[b] NPJSC "Shakarim University of Semey", Semey, Kazakhstan
[c] National Nuclear Center of the Republic of Kazakhstan, Kurchatov, Kazakhstan

Abstract

A neutronic model of the WWER-1000 reactor has been developed. The reactor block of the B-320 series, which is the most common among NPPs with the WWER type reactors, was selected for the modeling. The modeling was performed using the MCNP6 software. A three-dimensional model of the core has been developed, which fully corresponds to the reactor plant, both in terms of geometric parameters and material composition. The fuel assemblies and rods of the reactor control and protection system have been assembled into appropriate groups. The following opportunities have been implemented in the neutronic model: modeling of various critical reactor states; reactor power control; boron control; efficiency of individual rods and their groups. Preliminary calculations have been performed to substantiate the model operability. The integral and differential efficiency of the control protection systems, temperature feedback of reactivity, the Doppler coefficient, coolant density and boric acid concentration have been also studied.

Keywords: Neutronic model, WWER-1000, Fuel element, FA, Core, MCNP, CPS

1. Introduction

Neutron-physical modelling of nuclear power plants is an important aspect of scientific and technical support for the development of nuclear energy in the Republic of Kazakhstan. It is important for the Kazakh specialists to master tools and methods that will ensure quality verification of nuclear reactor characteristics declared by potential suppliers of reactor technologies, Will contribute to the organization of future efficient and stable operation of the NPP, as well as to the expansion of knowledge in the field of physics modelling of reactor plants.

Currently, Kazakh scientists, primarily employees of the National Nuclear Center of the Republic of Kazakhstan, have acquired significant competencies in numerical modeling of neutron-physical and thermodynamic processes in the IVG.1 M and IGR nuclear research reactors. The data obtained were used in the implementation of the project to convert cores to low-enrichment fuel [1,2], as well as in the preparation of in-pile experiments [3—7].

Today, the Republic of Kazakhstan stands on the threshold of a decision to build the first nuclear power plant [8]. The WWER-1000 reactor, or water—water power reactor, is one of the most common types of nuclear reactors designed for electricity generation. This reactor has a representative data set available to study the physics of pressurised water reactors in detail. In this context, it is appropriate to test methods and approaches for numerical modelling of power reactors to be carried out on the basis of this installation. The nominal electrical capacity of this reactor is 1000 MW, and thermal - 3000 MW. The water in this reactor performs three functions: heat carrier, neutron retarder and neutron reflector [9—12].

The development of the WWER-1000 reactor neutronic model, in particular the B-320 series reactor

Received 3 December 2024; revised 27 May 2025; accepted 6 June 2025.
Available online 30 June 2025

* Corresponding author at: "Institute of Atomic Energy" RSE NNC RK, Kurchatov, Kazakhstan.
E-mail address: seken@nnc.kz (D.M. Seken).

https://doi.org/10.69912/2616-8537.1248

unit, was carried out using the MCNP6 software. This model includes a three-dimensional representation of the reactor core, which exactly corresponds to the real installation in terms of geometric parameters and material composition.

The determination of kinetic parameters is of great importance in calculations of reactor physics for the transient reactivity analysis, safety and control of nuclear reactors. The kinetic parameters are the effective fraction of delayed neutrons, the lifetime of fast neutrons, and the neutron generation time.

One of the important parameters determining the reactor safe and stable operation is the calculation of the reactivity margin and the effect of the control and protection system (CPS) and boron control on the reactivity margin. CPS plays a key role in ensuring the WWER-1000 reactor stability and maintaining the required level of the reactivity margin. The CPS automatically reacts to changes in the reactor operating conditions, adjusting the control parameters to ensure safe and efficient operation. Real-time reactor control requires high accuracy and reliability of the CPS operation, especially under high loads and variable operating.

Boron control also plays an important role in ensuring the reactor safety. Boron is used to control the neutron flux, regulating its intensity and providing control over the process of nuclear fission. This allows the reactor to maintain optimal operating conditions and prevent possible emergencies.

In this paper, modeling of the core of the WWER-1000 reactor with the MCNP will be considered and the effect of the boron control and CPS on the reactivity margin will be analyzed. The integral and differential efficiency of the CPS, temperature feedback of reactivity, coolant density, boric acid concentration and Doppler coefficient have been studied. All calculations have been compared with the experimental and references data to conclude that the developed neutronic model is correct.

2. Object of research

The WWER-1000 reactor core is the central part of the reactor, where nuclear fission and a controlled chain reaction occur and it is composed of 163 fuel assemblies, each of which has 312 fuel elements. The main structural characteristics of the core are shown in Table 1 [13].

The first fuel loading of the reactor core is formed from the FAs of five types (Fig. 1):

- FA13AU – FA with 1.3 % (^{235}U) fuel enrichment;
- FA22AU – FA with 2.2 % (^{235}U) fuel enrichment;
- FA30AV5 – 303 fuel elements with 3.0 % (^{235}U) fuel enrichment, 9 fuel elements with 2.4 % (^{235}U) fuel enrichment and 5 % gadolinium oxide content;
- FA39AWU – 243 fuel elements with 4.0 % (^{235}U) fuel enrichment, 60 fuel elements with 3.6 % (^{235}U) fuel enrichment, 9 fuel elements with 3.3% (^{235}U) fuel enrichment and 5 % gadolinium oxide content;
- FA390GO – 240 fuel elements with 4.0 % (^{235}U) fuel enrichment, 66 fuel elements with 3.6 % (^{235}U) fuel enrichment, 6 fuel rods with 3.3 % (^{235}U) fuel enrichment and 5 % gadolinium oxide content [14].

Table 1. Main structural characteristics of the WWER-1000 reactor core.

Parameter name	Parameter value
The outer radius of the reactor vessel, mm	2267.5
The inner radius of the reactor vessel, mm	2068.0
The outer radius of the reactor barrel, mm	1810.0
The outer radius of the reactor baffle, mm	1742.5
The total number of the FAs in the core, pcs	163
The number of the FAs with CPS AR, pcs	61
The pitch between the FAs, mm	236

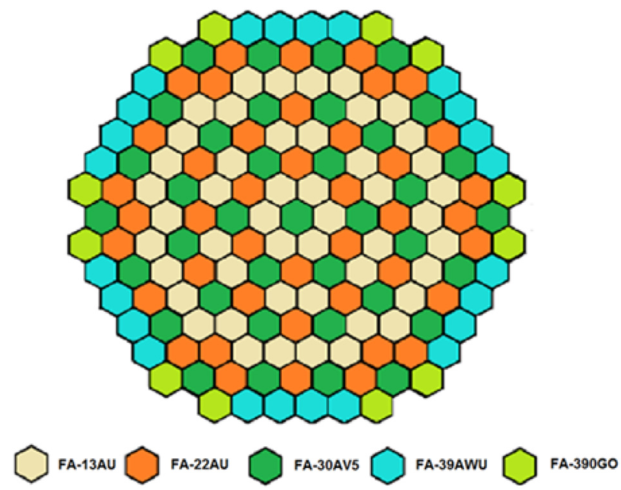

Fig. 1. The first reactor fuel cycle.

The fuel assembly (FA) consists of a power frame, a beam of fuel elements, a head and a bottom nozzle. The FA end parts are used to fix the cassette in the core setting sockets. The upper end part (head) provides interaction with the reactor inner devices and the FA compression from surfacing, as well as a detachable connection to the FA frame. The lower end part (bottom nozzle) provides a predetermined location of the cassette in the core, as well as the coolant path organization.

In the guide tubes, the drive can, depending on the position of the cassette in the core, move a beam of 18 absorber rods (ARs) of the control and protection system control rod, the AR core is made of a dispersion material [15]. Fig. 2 shows a dimensional drawing of the FA with the main dimensions. The main characteristics of the FAs are given in Table 2 [16].

The fuel element in Fig. 3 consists of a sealed shell, inside which the fuel is placed and the fission products are localized. Cylindrical uranium dioxide tablets with a density of 10400 kg/m3, each with an outer diameter of 7.53 mm and a height of 20 mm, are placed in the fuel rod. The total length of the fuel column is 3530 mm (extension by ~ 30 mm is possible when operating at power). In the middle of the tablet there is a hole with a diameter of 1.4 mm, the edges are chamfered. The gap between the tablet and the shell, as well as the central hole, are designed to allow the tablet to increase as a result of radiation swelling. For spatial fixation of the fuel column and ensuring its continuity, a fixing element (spring, split sleeve, etc.) is placed in the fuel element. The fuel element shell, made of zirconium alloy, provides the required mechanical strength of the structure, its dimensional stability, and also protects nuclear fuel and fission products from the corrosive and erosive effects of the coolant. The main characteristics of fuel rods are shown in Table 3.

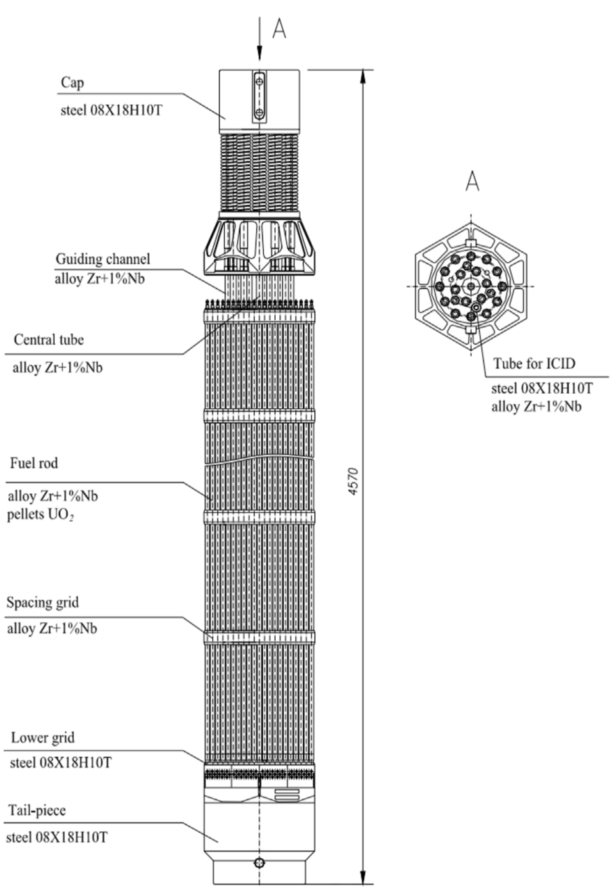

Fig. 2. Fuel assembly.

Table 2. Main characteristics of the WWER-1000 reactor FA.

Parameter	Value
The FA size (turnkey), mm	234
The number of the fuel rods in the FA	312
The method of placing the fuel rods	Uniformly triangular
The pitch between the fuel rods, mm	12.75
The fuel rod diameter, mm	9.1
The number of guide channels in the FA, pcs	18
The central tube (frame) for placement of the energy measurement sensors, pcs	1
The number of absorber rods in the beam, pcs	18
The material of the tubes of the guide channels	Stainless steel
The central tube material	Zr+1 %Nb alloy
The central tube size, mm	Ø11 × 0.8
The size of the tubes of the guide channels, mm	Ø12.6 × 0.8

The loading of the WWER-1000 with uranium is approximately 70 tons, the average enrichment in the core in the steady—state mode is 3—3.3 %, which approximately corresponds to 2100 kg of ^{235}U.

Reactor power is regulated by the control and protection system (CPS) — by changing the position of clusters of rods with absorbing elements (AEs) in the core, as well as by changing the concentration of boric acid in the water of the primary circuit.

In the standard V-320 project, 61 clusters of the CPS control rod (CR) are installed at the WWER-1000 reactor, divided into 10 groups, one of which is used for operational control, 9 others as emergency protection and solving some specific tasks, for example, suppression of xenon oscillations. Each cluster contains 18 absorbing rods.

The AEs are moved (Fig. 4) in the guide tubes with a size of 12.6 × 0.8 mm, called the CPS guide channels. The radial annular gap between the AE and the guide tube inner surface is 0.9 mm [17].

The main characteristics of the CPS CR are given in Table 4.

Fig. 5 shows the numbering of the FAs, the placement of 61 CPS CRs in the WWER-1000 core and the location of the loops.

3. Methods of research

One of the main tools for studying the neutron-physical characteristics of systems is the MCNP (Monte Carlo N-Particle) software package [18] that uses estimated nuclear data libraries ENDF/B-VII.0 [19] for calculation of the neutron transport equasions.

The MCNP input file consists of three main sections: cell maps, surface maps, and data maps. The geometry and material parameters defining the system structure

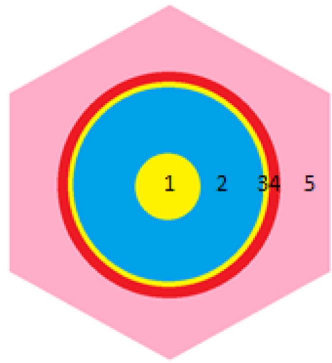

1 – central hole, 2 – fuel, 3 – gap between the fuel and cladding, 4 – cladding, 5 – moderator.

Fig. 3. Horizontal section of the fuel element.

Table 3. Main characteristics of the WWER-1000 reactor fuel elements.

The radius of the fuel element central hole, mm	0.7
The fuel outer radius, mm	3.765
The inner radius of the fuel element cladding, mm	3.9
The outer radius of the fuel element cladding, mm	4.55
Enrichment, %	1.3–2.2 – 3.0–3.6 – 4
The fuel element height, mm	3530
The cladding material	Zr + 1 % Nb
The fuel weight in 1 fuel element, kg	1.575
The fuel	UO_2
The fuel density, kg/m3	10400
The moderator	H_2O
The gas, filling the gap between the pellet and cladding	He

are input into the cell maps. Each cell is described by a number, material, density, and associated surfaces. The surface maps define geometric surfaces that divide the space into different areas. These surfaces can be used for defining the cell edges and the system shape. The data maps contain the parameters for calculations, such as the number of neutrons per a cycle, the initial value of the fission factor, and other modeling settings.

The neutron fission factor K_{eff} is a key parameter for determining the state of a chain reaction in a nuclear reactor. Three calculation options have been considered to compare the effective neutron fission factor and the fraction of the delayed neutrons with the data from the source for the reactor model.

For critical neutron calculation the following initial parameters are used: number of neutrons — 10 000 000, initial k_{eff} — 1.00, number of cycles skipped — 50, total number of cycles 200. The calculation error is around ±0.00002–0.00003 (or ±0.002–0.003 %), which is considered to be an acceptable level of accuracy for neutron-physical calculations.

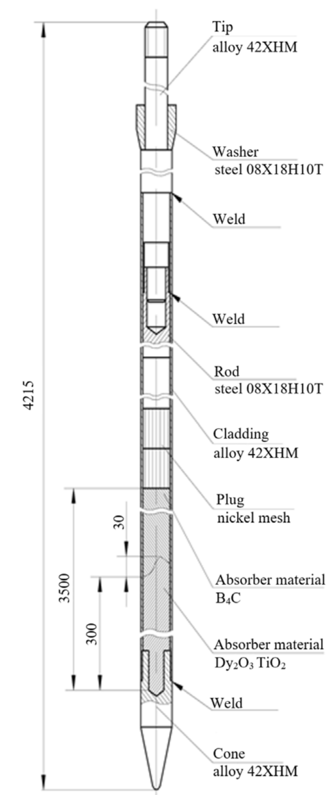

Fig. 4. Absorber element.

1. The calculation of the reactivity margin based on K_{eff} at the first fuel loading into the reactor is carried out without the use of a control and protection system and without boron control. The temperature of the coolant and fuel is equal to 300 K in this version. The reactor reactivity (ρ) can be calculated using the neutron fission factor K_{eff} according to the formula:

$$\rho = \left(1 - \frac{1}{K_{eff}}\right)/0.0064 \tag{1}$$

Table 4. Main characteristics of the CPS CR.

Parameter name	Parameter value
The number of AEs in the CPS CR	18
The absorber material	
- Upper part	B_4C
- Lower part	$Dy_2O_3 \times TiO_2$
The absorber height, mm	
- Total	3530
- Upper part	3230
- Lower part	300
The absorber material density, kg/m3	
- Upper part	1700
- Lower part	4900
The outer diamter of the AE cladding, mm	8.2
The AE cladding thickness, mm	0.6
The cladding material	Stainless steel
The number of the CPS rods, pcs	61

Here, ρ — reactivity, K_{eff} — neutron fission factor, 0.0064 — effective fraction of delayed neutrons.

2. The calculation with the CPS fully introduced into the core and without boron control with the fuel and coolant temperature of 300 K. The calculation is necessary to evaluate the efficiency of the reactor reactor control system under these conditions.

3. The calculation with boron control

The boron control is changing the boric acid concentration in the water of the primary circuit. The main purpose of the boron control is to compensate for slow changes in the reactivity during reactor operation.

At the operation initial stage, the boric acid concentration is 0—16 g/kg (H_2O) for compensating the large margin of the fuel reactivity, which is about 30β. As the fuel burns out, the boric acid concentration gradually decreases in order to maintain the stable neutron power.

At this stage, the boric acid concentration is 6 g/kg (H_2O), and all groups of the control rods are removed from the core. The temperature of the fuel and coolant is 300 K each.

4. Neutronic model of the core

Fig. 6 shows a complete geometric model of the reactor core in the MCNP (VisEd) visual editor. The model includes all the key components of the core, such as 163 fuel assemblies with the fuel elements, reflectors, control and protection systems. The use of

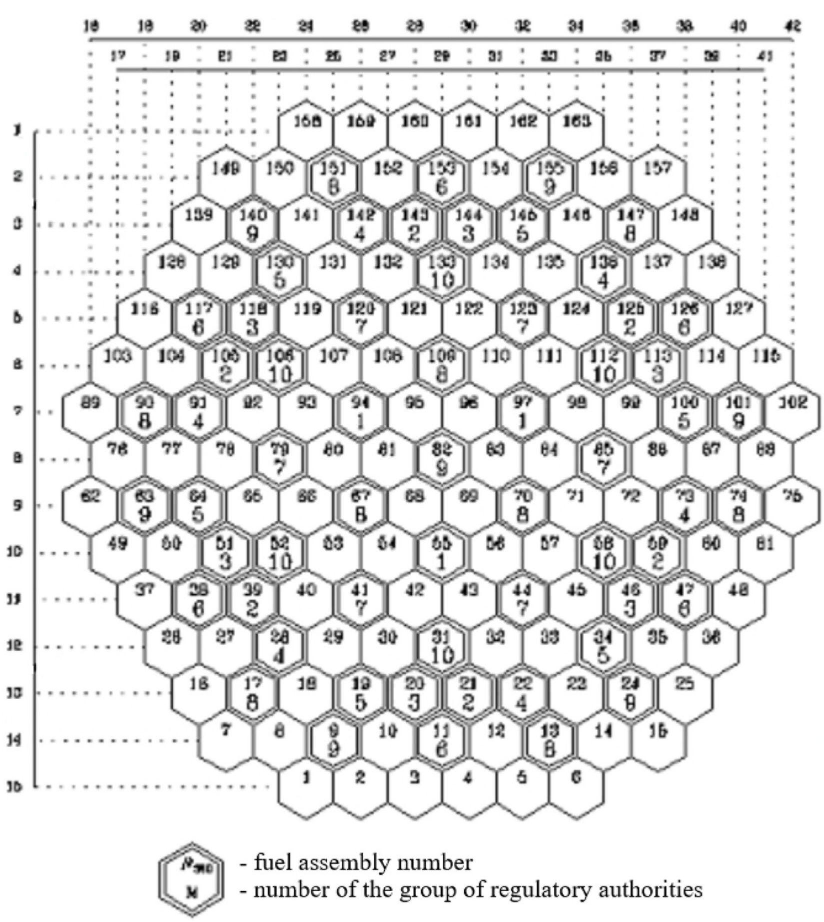

Fig. 5. —Numbering of the FAs and the placement of 61 CPS CRs in the WWER-1000 core.

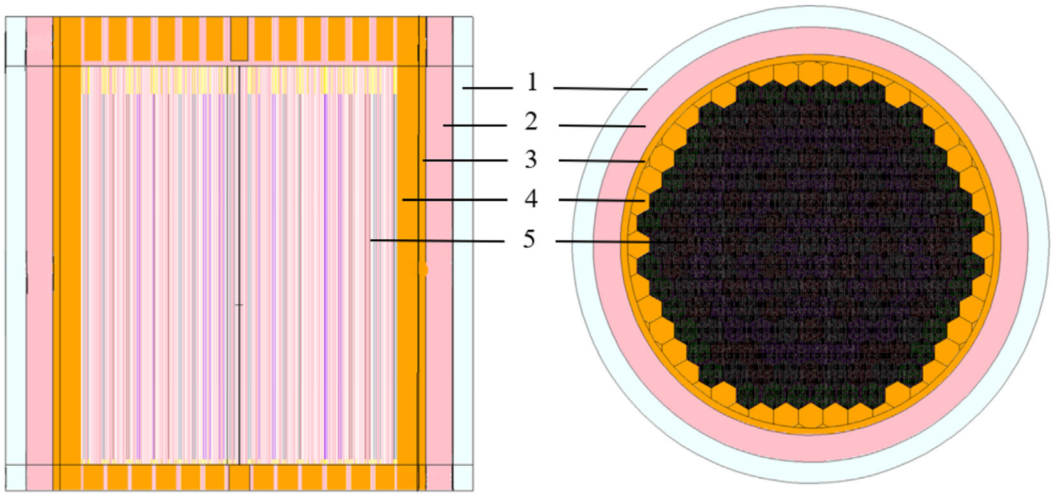

1 – vessel, 2 – reflector, 3 – barrel, 4 – baffle, 5 – active core.

Fig. 6. Graphical representation of the reactor design model.

VisEd allows visualizing the structure and layout of the reactor, which facilitates the construction of a model and its debugging for the safe and efficient operation of the WWER-1000/B320.

Each fuel assembly has a different arrangement of the fuel elements as shown in Fig. 7.

Fig. 8 shows a complete geometric model of the fuel element with 3.0 % fuel enrichment and 2.4 % uranium gadoline fuel element of the WWER-1000/B320 reactor in the MCNP (VisEd) visual editor. The enrichment of gadolinium oxide in U-Gd is 5.0 %.

5. Calculation results

The neutron fission factor at the first fuel loading without the CPS and boron control was 1.17695 (±0.00003). Thus, the reactor reactivity margin was 23.5β [20,21].

The neutron fission factor was 1.11358 (±0.00002) and the reactivity was 15.9β with the CPS completely dropped without the boron control.

The neutron fission factor was 1.00128 (±0.00002) and the reactor reactivity was 0.21β with the boron control.

Thereby, it requires the effective using of the control systems and adding the boric acid to the water in order to reduce the reactor reactivity during the first fuel loading. It is possible to adjust the reactivity throughout the entire operating cycle ensuring the reactor stable operation by immersing the CPS into the core and adjusting the boric acid.

The value of the parameters of the delayed neutrons during the boron control is given in Table 5, where l_i is the average lifetime of the emitter nuclei, β_i is the fracture of the delayed neutrons, λ_i are the radioactive decay constants of the i-th group. The reactor kinetics depends on the properties of the groups of the delayed neutrons of the fissile material. On a more precise examination, six groups of delayed neutrons are taken into account.

The delayed neutrons play a key role in the reactor reactivity controll. They provide additional time for the reactor to balance the reactivity which is critical for safety. Precise values of the parameters, such as the average lifetime of the emitter nuclei (l_i), the fraction of the delayed neutrons (β_i), and the radioactive decay constants (λ_i), make it possible to forecast the reactor behavior more accurately.

One of the methods of testing the reactor model is to compare the effective fraction of the delayed neutrons, calculated using the MCNP_NNC code, with the references data. Table 6 shows the calculated effective fraction of the delayed neutrons in comparison with the references data.

Table 6 illustrates that the calculated effective fraction of the delayed neutrons correlates with the given reference data, which confirms the model reliability.

6. Model verification

Figs. 9 and 10 show the integral and differential efficiency of the working (No. 10) group of the CPS when they were removed from the core with the pitch of 350 mm. CPS groups No. 1—9 were removed from the core where the boric acid concentration was 4 g/kg (H_2O), and the temperature of the coolant and fuel was 600 K (the results of the K_{eff} and the changing parameters of the reactor model are shown in Table 7).

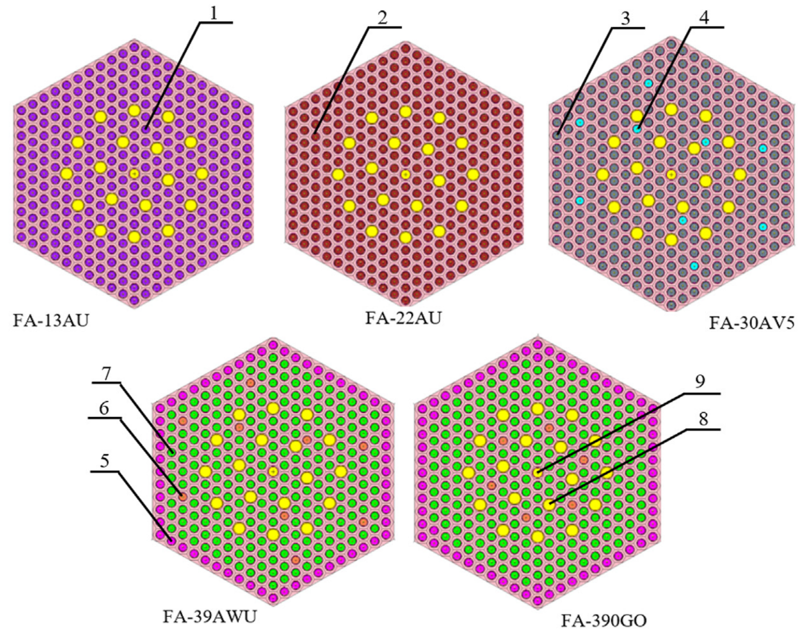

1 – fuel element with 1.3 % fuel enrichment, 2 – fuel element with 2.2 % fuel enrichment, 3 – fuel element with 3.0 % fuel enrichment, 4 – fuel element with 2.4 % fuel enrichment and 5 % gadolinium oxide content, 5 – fuel element with 3.6 % fuel enrichment, 6 – fuel element with 3.3 % fuel enrichment and 5 % gadolinium oxide content, 7 – fuel element with 4.0 % fuel enrichment, 8 – guide channel, 9 – central channel.

Fig. 7. Arrangement of fuel elements in the FAs of different types: 13AU, 22AU, 30AV5, 39AWU, and 390GO.

The comparison of the calculated MCNP_NNC data with the reference [23], where there are the experimental and calculated data of the RAINBOW software package, is shown.

The comparison of the measured values with the data obtained during modeling with MCNP_NNC was performed for the CPS group No. 10 during the withdrawal. The absolute error of the experimental and Rainbow calculated data was 0.009 for the integral characteristic of the CPS group No. 10. And it was 0.02 for the data from the experiment and calculation of the MCNP_NNC.

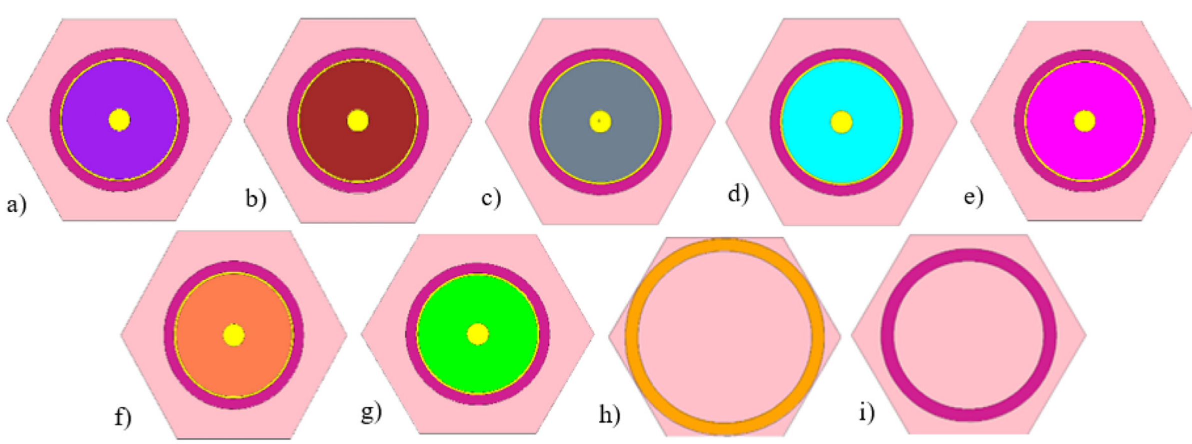

a) fuel element with UO_2 (1.3 %) fuel, b) fuel element with UO_2 (2.2 %) fuel, c) fuel element with UO_2 (3.0 %) fuel, d) fuel element with UO_2 (2.4 %) Gd_2O_3 fuel, e) fuel element with UO_2 (3.6 %) fuel, f) fuel element with UO_2 (3.3 %) Gd_2O_3 fuel, g) fuel element with UO_2 (4.0 %), h) guide channel, i) central channel.

Fig. 8. Fuel element and channel model.

Table 5. Parameters of delayed neutrons.

Neutrons group number (i)	1	2	3	4	5	6
Fraction of the total number of delayed neutrons (β_i)	0.00020	0.00113	0.00110	0.00318	0.00103	0.00035
Decay constant (λ_i), s^{-1}	0.01249	0.03168	0.11007	0.32014	1.34664	8.85678
Average life time (l_i), s	55.49294	21.88179	6.29715	2.16516	0.51472	0.07826

Table 6. Calculated effective fraction of the delayed neutrons in comparison with the references data.

	$K_{eff} \pm \sigma$ (MCNP_NNC calculation)	β_{eff} (MCNP_NNC calculation)	β_{eff} (references data)
Variant 1	1.17695 ± 0.00003	0.00686 ± 0.00006	0.00724 [14]
Variant 2	1.11358 ± 0.00002	0.00684 ± 0.00007	0.00639 [22]
Variant 3	1.00900 ± 0.00004	0.00698 ± 0.00006	

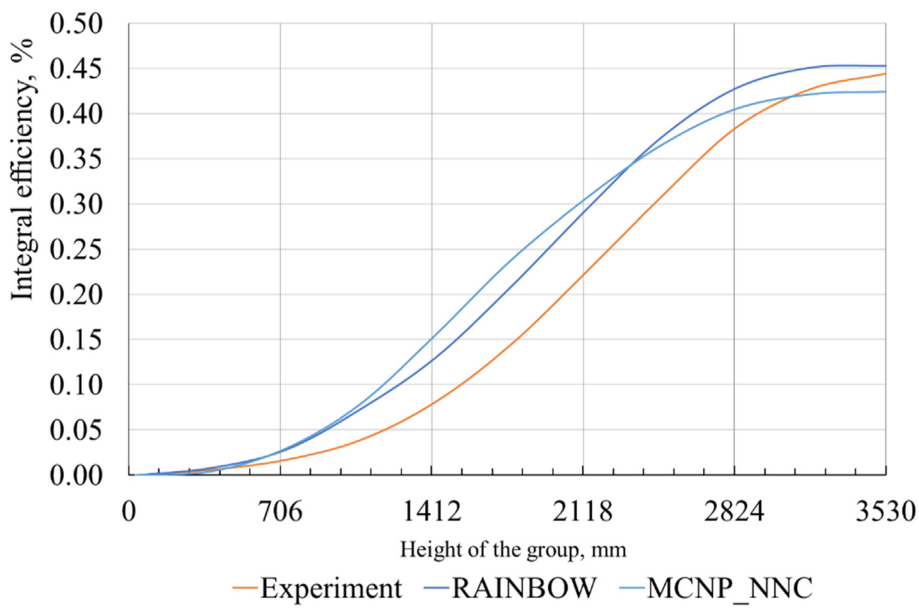

Fig. 9. CPS integral efficiency.

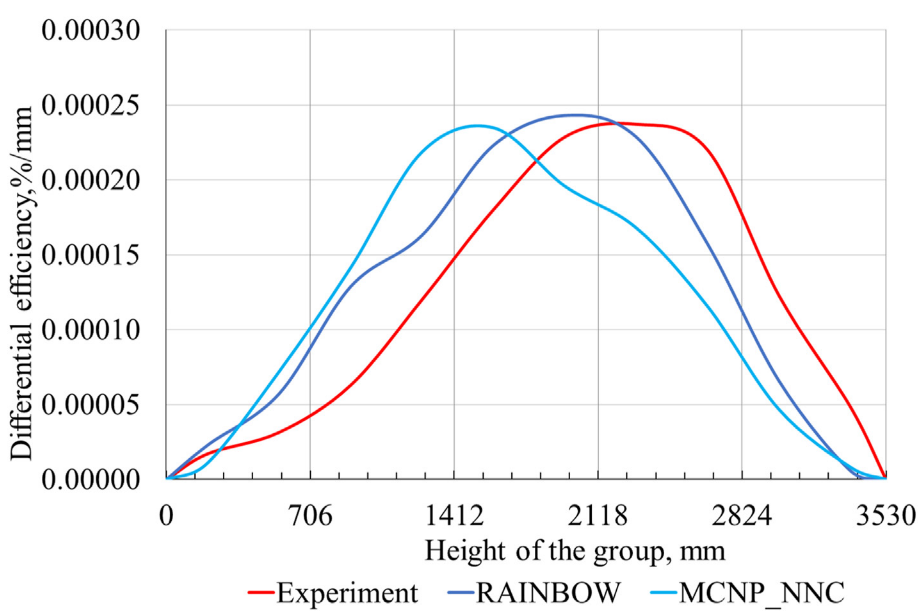

Fig. 10. CPS differential efficiency.

Table 7. Integral and differential efficiency.

Calculation	Coolant density, kg/m^3	Fuel temperature, K	Coolant temperature, K	CPS No.10[a], mm	Boric acid, g/kg (H_2O)	K_{eff}
1	700	600	600	3530	4	1.01514(2)
2	700	600	600	3180	4	1.01518(3)
3	700	600	600	2830	4	1.01544(2)
4	700	600	600	2480	4	1.01595(3)
5	700	600	600	2130	4	1.01674(2)
6	700	600	600	1780	4	1.01759(3)
7	700	600	600	1430	4	1.01830(2)
8	700	600	600	1080	4	1.01891(2)
9	700	600	600	730	4	1.01933(2)
10	700	600	600	380	4	1.01950(2)
11	700	600	600	30	4	1.01953(2)

[a] 353-CPS No.10 is completely in the core, 0-CPS No.10 is above the core.

The differential efficiency of a movable absorber at a given position «H» along the height of the reactor core is defined as the amount of positive reactivity released when it is raised by one unit of length from the specified position «H». This parameter determines how effectively the rod compensates for reactivity perturbations, ensuring safe and stable reactor operation. It is used in the design and calibration of the CPS, rod placement optimization, and fuel burnup management because the efficiency depends on the insertion depth and core condition.

The relative error of the differential characteristic peak was 2.35 % for the value of the experiment and the Rainbow software package. The relative error for the experiment and MCNP_NNC was 1.028 %.

Fig. 11 shows a comparison of the results between the MCNP_NNC calculated data, the Nguyen Huu Tiep (MCNP5) data from the reference [24] and the SRAC software package. In these variants, the temperature of the moderator was assumed to be equal to 600 K, the boric acid and CPS CR were not modeled (Table 8). The fuel temperature changed step by step from 600 to 1200 K (each step is 100 K). As Fig. 11 shows, it was found that K_{eff} decreases with the fuel temperature increasing, which is the expected behavior.

First, the change in the reactivity was calculated using the Equation (2) to compare the Doppler coefficient.

$$\Delta\rho = \frac{K_{eff}^{T_2} - K_{eff}^{T_1}}{K_{eff}^{T_2} \cdot K_{eff}^{T_1}} \tag{2}$$

here, $K_{eff}^{T_2}$ and $K_{eff}^{T_1}$ correspond to the effective neutron fission factor for temperatures T2 and T1. The Doppler coefficient (D_c) was then calculated as the ratio of the change in reactivity to the change in the fuel temperature using Equation (3) and expressed in pcm/K (1 pcm $= 10^{-5}$).

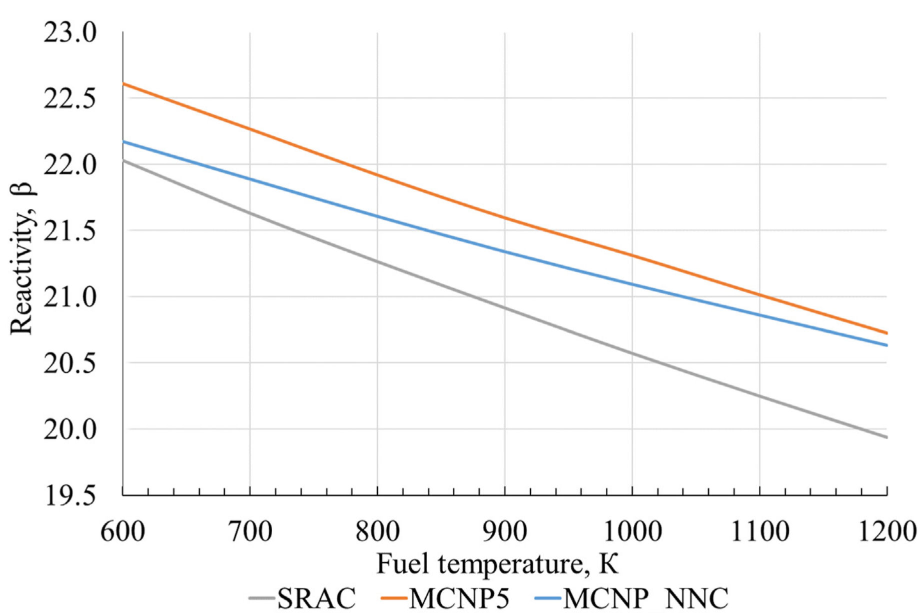

Fig. 11. Change in reactivity depending on the change in the fuel temperature.

Table 8. Change of the reactivity depending on the fuel temperature change.

Calculation	Coolant density, kg/m^3	Fuel temperature, K	Coolant temperature, K	CPS No.10, mm	Boric acid, g/kg (H_2O)	K_{eff}
1	1000	600	300	0	0	1.16839(6)
2	1000	700	300	0	0	1.16588(6)
3	1000	800	300	0	0	1.16340(6)
4	1000	900	300	0	0	1.16106(6)
5	1000	1000	300	0	0	1.15891(6)
6	1000	1100	300	0	0	1.15689(6)
7	1000	1200	300	0	0	1.15491(6)

$$D_c = \frac{\Delta\rho}{\Delta T} \tag{3}$$

here, ΔT is the fuel temperature change (ΔT = 600 K in this case).

It was found that the reactivity decrease (Doppler effect) due to the temperature increase from 600 K to 1200 K was −2.03969 pcm/K (MCNP5), −2.263647 pcm/K (SRAC) and −1.665 pcm/K (MCNP_NNC). This result corresponds to some calculation results for a light-water reactor and does not exceed the values recommended in ISAR [25] (from −3.3 to −1.7 pcm/K).

Fig. 12 shows a comparison of the calculated data with the reference [26] (the SAPPHIRE program, where the fuel concentration is higher since the fuel load includes the FAs with an enrichment of 3.3 % and 4.4 %, as well as with grouping with the fuel elements with an enrichment of 3.6 %.) when the coolant density changes. The calculation of the fission factor in the range of changes in coolant density from 0.01 to 1000 kg/m^3 (boric acid concentration was 16 g/kg (H_2O), the coolant and fuel temperature was 300 K, Table 9) was carried out for the fully fueled cores at the beginning of fuel loading. The boric acid with a sufficiently high concentration (16 g/kg H_2O) is used to ensure subcriticality in an emergency or overload. The results of K_{eff} calculation are shown in Fig. 12.

The absolute error of the dependence of effective neutron fission factor on the coolant density of 1000 kg/m^3 was 0.0872.

The calculation of the effective fission factor in the boric acid concentration range from 16.0 g/kg (H_2O) to zero was carried out for the primary fuel loading of the cores. The results of K_{eff} calculation are shown in Table 10 and Fig. 13 in comparison with the reference [21].

The absolute error for the dependence of the effective neutron fission factor on the boric acid concentration in the coolant for the calculation results according to the SAPPHIRE and MCNP_NNC codes is 0.04237 at 0 g/kg (H_2O) and 0.095 at 16 g/kg (H_2O).

The calculation results show that at the start of the campaign, the criticality is achieved at a boric acid concentration of 6.4 g/kg (H_2O). The complete removal

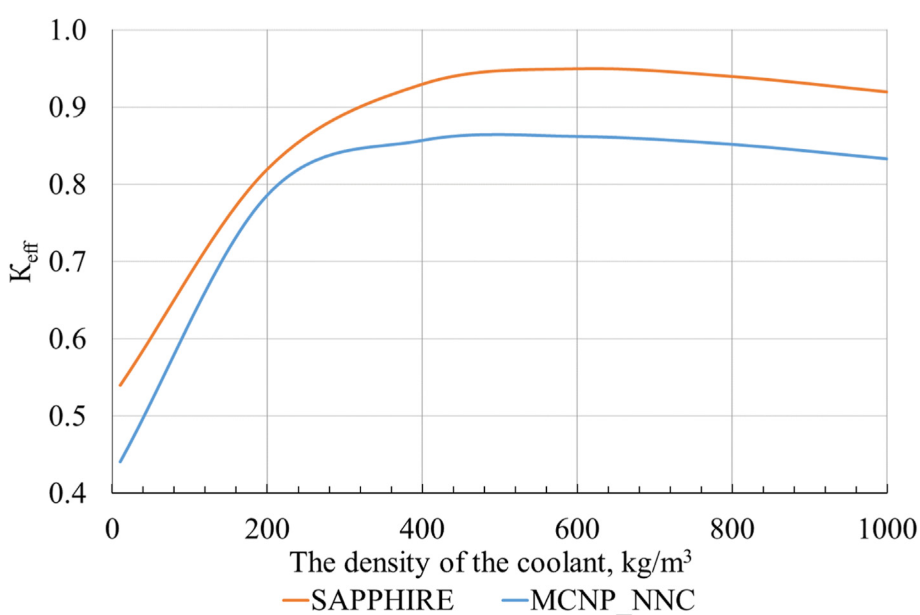

Fig. 12. Dependence of the effective fission factor on the coolant density with the boric acid concentration 16 g/kg (H_2O).

Table 9. Dependence of the effective fission factor on the coolant density.

Calculation	Coolant density, kg/m^3	Fuel temperature, K	Coolant temperature, K	CPS No.10, mm	Boric acid, g/kg (H_2O)	K_{eff}
1	10	300	300	0	16	0.44057(3)
2	200	300	300	0	16	0.78593(4)
3	400	300	300	0	16	0.85662(5)
4	600	300	300	0	16	0.86178(6)
5	800	300	300	0	16	0.85154(5)
6	1000	300	300	0	16	0.83280(5)

Table 10. Dependence of the effective fission factor on the boric acid concentration in the coolant.

Calculation	Coolant density, kg/m^3	Fuel temperature, K	Coolant temperature, K	CPS No.10, mm	Boric acid, g/kg (H_2O)	K_{eff}
1	1000	300	300	0	0	1.17763(6)
2	1000	300	300	0	2	1.11241(6)
3	1000	300	300	0	4	1.05702(6)
4	1000	300	300	0	6	1.00910(6)
5	1000	300	300	0	8	0.96666(6)
6	1000	300	300	0	10	0.92865(6)
7	1000	300	300	0	12	0.89444(5)
8	1000	300	300	0	14	0.86337(5)
9	1000	300	300	0	16	0.83497(6)

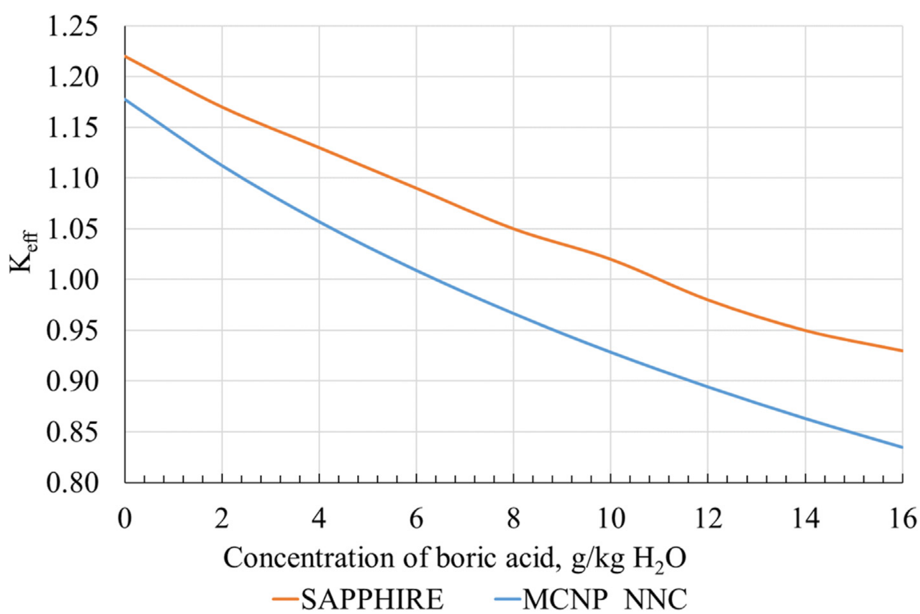

Fig. 13. Dependence of the effective fission factor on the boric acid concentration in the coolant.

of the boric acid from the coolant leads to an increase in the fission factory up to 1.17763.

The calculation results confirm the suitability of modeling neutronic processes occurring in the reactor core using the MCNP software package.

7. Conclusion

A neutronic model of the WWER-1000 reactor facility was developed and verified using the MCNP6 software package. The model was created considering the key geometrical and material characteristics of the fuel and core components. It allows for accurate calculations of the core's key parameters at different stages of the fuel campaign.

The performed simulations showed that at the beginning of the fuel cycle, without the use of control rods or boron regulation, the neutron multiplication factor is 1.17695 (±0.00003), which corresponds to a reactivity margin of approximately 23.5β.

With full insertion of the control rods, the value decreases to 1.11358 (±0.00002), and the reactivity drops to 15.9β. When boron regulation is applied, the multiplication factor is 1.00128 (±0.00002), indicating an almost critical state of the reactor (reactivity of 0.21β). These results confirm the necessity of comprehensive application of control systems for reactivity management and safe reactor operation.

An evaluation of the effective delayed neutron fraction yielded ≈0.0068—0.0070, which is in good agreement with the reference range (0.0064—0.0072), confirming the correctness of the reactor kinetics description.

Integral and differential characteristics were obtained for one of the control rod groups (No. 10), with a deviation from experimental data not exceeding 2 %, which further indicates the adequacy of the model. The calculated Doppler coefficient was −1.665 pcm/K, falling within the IAEA-recommended range (−3.3 to −1.7 pcm/K). It was also demonstrated that increasing fuel temperature from 600 to 1200 K and changing the coolant density from 10 to 1000 kg/m^3 significantly affect reactor criticality, as does varying boric acid concentration from 16 to 0 g/kg (at zero concentration, $K_{eff} = 1.17763$).

Thus, the calculations confirm that the developed model accurately reflects the physical processes in the WWER-1000 core and can be used for analysis, design, and optimization of operating modes, as well as for verification of new calculation methods. The model provides a high level of consistency with experimental and published data and can be applied to justify the safety and efficiency of reactor facility operation.

The work was carried out within the framework of the project of the Science Committee of the Ministry of Education and Science of the Republic of Kazakhstan “Research in support of the creation and safe operation of a nuclear power plant in the Republic of Kazakhstan” (BR21882185).

Funding

The work was carried out within the framework of the project of the Science Committee of the Ministry of Education and Science of the Republic of Kazakhstan “Research in support of the creation and safe operation of a nuclear power plant in the Republic of Kazakhstan” (BR21882185).

Conflicts of interest

The authors declare no conflicts of interest.

References

[1] R. Irkimbekov, et al., Energies 16 (2023) 932, https://doi.org/10.3390/en16020932.
[2] R.A. Irkimbekov, et al., Nucl. Eng. Technol. 55 (2023) 4, https://doi.org/10.1016/j.net.2022.12.012.
[3] E. Batyrbekov, et al., Ann. Nucl. Energy 182 (2023) 109582, https://doi.org/10.1016/j.anucene.2022.109582.
[4] G.A. Vityuk, et al., Bull. NNC RK 3 (2017) 24—30 (In Russian), https://www.nnc.kz/media/bulletin/files/3jsvHtpUr4.pdf.
[5] A.D. Vurim, et al., Bull. NNC RK 1 (2015) 55—60 (In Russian), https://www.nnc.kz/media/bulletin/files/HnplApAnHy.pdf.
[6] B.E. Bekmagambetova, et al., Bull. NNC RK 3 (2014) 36—39 (In Russian), https://www.nnc.kz/media/bulletin/files/dy0mDZ3yu0.pdf.
[7] G.A. Vityuk, et al., Eurasian J. Phys. Funct. Mat. 6 (2022) 198—212, https://doi.org/10.32523/ejpfm.2022060305.
[8] E. Batyrbekov, et al., Energies 17 (2024) 5788, https://doi.org/10.3390/en17225788.
[9] A.I. Elazaka, et al., Int. J. Energy Res. 45 (2021), https://doi.org/10.1002/er.6494.
[10] S.T. Leskin, et al., Physical Characteristics and Design of the VVER-1000 Reactor: Textbook, NRNU MEPhI, Moscow, 2011, p. 116 (In Russian).
[11] M.I. Hossain, et al., Nucl. Eng. Technol. 8 (2022) 1—11, https://doi.org/10.3897/nucet.8.78447.
[12] A. Safavi, et al., Nucl. Eng. Technol. 52 (2020) 1603—1610, https://doi.org/10.1016/j.net.2020.01.024.
[13] S.B. Ryznov, et al., WWER-TYPE Reactors of Russian Design: Handbook of Nuclear Engineering, Springer, 2010, p. 72, https://doi.org/10.1007/978-0-387-98149-9_20.
[14] H. Louis, J. Nucl. Part. Phys. 11 (2021) 15—26, https://doi.org/10.5923/j.jnpp.20211101.03.
[15] G.N. Kolpakov, et al., Designs of Fuel Elements, Channels and Cores of Power Reactors, 2009, p. 118 (In Russian).
[16] S.A. Andrushchenko, et al., NPPt with a WWER-1000 reactor, in: From the Physical Foundations of Operation to the Evolution of the Project, Logos, Moscow, 2010, p. 604 (In Russian), https://elib.biblioatom.ru/text/andrushechko_aes-s-reaktorom-vver-1000_2010/p130/.
[17] G.L. Ponomarenko, et al., Proceedings of the 6th International Scientific and Technical Conference “Ensuring the Safety of NPPs with WWER”, Podolsk, 2009. No. 19. (In Russian), http://www.atominfo.ru/news/air6946.htm.
[18] MCNP6 Monte Carlo N—Particle Transport Code System, MCNP6.1, LANL, 2013.
[19] ENDF/B-VII.0: Next Generation Evaluated Nuclear Data Library for Nuclear Science and Technology. Nuclear Data Sheets, 2006.
[20] N.N. Alekseyev, Intelligent Energy Systems: Proceedings of the V International Youth Forum, Tomsk, 2, 2017, pp. 79—82 (In Russian).
[21] H.N. Tran, H.T.P. Hoang, P.H. Liem, Energy Proc. 131 (2017) 29—36, https://doi.org/10.1016/j.egypro.2017.09.442.
[22] Y.N. Nikulina, et al., Yaderna ta radiatsiyna bezpeka 1 (2018) 18—23 (In Russian), https://core.ac.uk/download/pdf/270038788.pdf.
[23] O.Yu. Kavun, A.I. Popykin, Issues of atomic science and technology, Series: Ensur. Safety Nucl. Power Plants 34 (2014) 93—98 (In Russian), https://www.elibrary.ru/download/elibrary_23050627_77918527.pdf.
[24] H.T. Nguyen, et al., Some neutronics calculations for the WWER-1000 reactors. https://inis.iaea.org/records/9x07e-fhj52/files/47065288.pdf?download=1, 2015.
[25] Risk Engineering LTD., Belene ISAR — Training course provided for Vietnam Atomic Energy Institute VINATOM, 2012. Sofia, Bulgaria, https://inis.iaea.org/records/9x07e-fhj52/files/47065288.pdf?download=1.
[26] A.E. Borisenkov, et al., Bull. SSTU 5 (2006) 82 (In Russian), https://www.sstu.ru/upload/medialibrary/dcf/04_20_2006.pdf#page=82.